www.czasopisma.pan.pl PAN www.journals.pan.pl

ARCHIVES of FOUNDRY ENGINEERING

ISSN (2299-2944)
Volume 2025
Issue 1/2025

121 – 128

10.24425/afe.2025.153781

14/1

Published quarterly as the organ of the Foundry Commission of the Polish Academy of Sciences

The Impact of Alloying Additives on the Shrinkage Processes and Corrosion Resistance of Lead-Free Casting Brasses

G. Radzioch [a, b, *], D. Bartocha [a], M. Kondracki [a]

[a] Department of Foundry Engineering, Silesian University of Technology, 7 Towarowa Str. 44-100 Gliwice, Poland
[b] Joint Doctoral School, Silesian University of Technology, 2A Akademicka Str. 44-100 Gliwice, Poland
* Corresponding author: e-mail: grzegorz.radzioch@polsl.pl

Received 05.08.2024; accepted in revised form 20.12.2024; available online 17.03.2025

Abstract

The article presents a comparative analysis of lead-free brass (CB771) and lead-containing brass (CB770). The study aimed to assess shrinkage processes and corrosion resistance. CB771 samples with modified chemical composition, enriched with zinc, aluminum and tin, were compared with CB770 samples in terms of casting shrinkage and susceptibility to dezincification. Dilatometric analysis revealed that different alloying additives affect shrinkage and dimensional stability at high temperatures in various ways. Aluminum and tin significantly improved resistance to dezincification, while the addition of zinc proved to be less effective. Microscopic examinations confirmed that alloys with aluminium and tin additives have a finer structure, which can translate to higher mechanical properties. The results suggest that lead-free alloys can replace traditional alloys in sanitary applications, reducing the negative impact of lead on the environment and public health.

Keywords: Lead-Free Brass, Dilatometric Analysis, Shrinkage, Corrosion resistant, Dezincification

1. Introduction

Copper-zinc alloys, known as brass, are used in the production of pipes, valves, and sanitary fittings due to their excellent corrosion resistance. CuZn alloys with a lead content of approximately 1.6% are particularly popular because of their good technological properties, such as castability and machinability. However, the toxic nature of lead is increasingly recognized by governments and health organizations around the world, leading to a reduction in the content of this element in products that come into contact with drinking water [1,2].

Reducing the lead content below 0.2% results in a significant decrease in casting properties (castability, reproducibility) and machinability. At the same time, there is an increased tendency to formation of shrinkage and surface defects [3-5].

The European Union Parliament, WHO, and members of the Joint Committee of the European Valve and Fitting Manufacturers Association of Four Member States (4MS) are introducing further restrictions on the allowable content of Pb and Ni in brass used in drinking water applications, promoting the development of new lead-free CuZn alloys [6,7]. To achieve the goal of gradually phasing out leaded brass from the infrastructure, it is necessary to expand the knowledge regarding lead-free CuZn alloys.

After casting, the metal undergoes continuous shrinkage in the liquid state, during solidification, and in the solid state during cooling. In certain temperature ranges, these changes exhibit a stepwise nature that is associated with phase transformations. In foundry practice, this phenomenon is known as casting shrinkage, encompassing all processes leading to reduction of casting dimensions during solidification and cooling relative to the mould cavity dimensions. Uncontrolled shrinkage processes can lead to

defects in castings, such as porosity, shrinkage cavities, cracks, and distortions.

Understanding total casting shrinkage is insufficient for a complete comprehension of this phenomenon; therefore, it is necessary to analyze dilatometric curves, which provide information on the magnitude and kinetics of shrinkage. To conduct such studies, a measurement setup was designed and constructed for the continuous registration of dimensional changes in the casting during solidification and cooling, based on the construction of the DO-01/P.ŚL foundry dilatometer [8].

Corrosion is a process of degradation of the material resulting from environmental interaction, which in the case of brass is complex due to its composition. Brass exhibits good anticorrosion properties, especially compared to steel or cast iron [9], thanks to the presence of copper, which corrodes slowly in neutral pH environments, such as saltwater. However, the presence of zinc, a metal less resistant to corrosion, makes brass susceptible to a specific form of corrosion known as dezincification, or selective leaching of zinc [10].

Dezincification initiates when brass is exposed to a corrosive environment containing aggressive substances such as chlorides, sulfates, and other salt solutions, typically found in marine environments or certain industrial applications. Key factors also include pH, oxygen content, and ambient temperature. Under such conditions, zinc, being more anodic than copper, preferentially dissolves from the brass matrix. The electrochemical potential difference between zinc and copper promotes selective leaching of zinc, leaving behind a porous copper structure often referred to as a 'dezincified layer.' This structure is significantly weaker and more brittle than the original alloy, making it prone to cracks and mechanical damage [11].

The rate and extent of dezincification are variable and depend on numerous factors, including alloy composition, presence of impurities, microstructure of the alloy, and environmental conditions such as the composition of the corrosive medium, temperature, and fluid dynamics. The microstructure of brass, particularly the size and shape of the grains, significantly affects the dezincification process. Alloys with larger grain boundary areas often exhibit higher rates of dezincification due to increased surface area exposed to corrosion. Furthermore, the presence of precipitates and inclusions can act as local cathodes, intensifying the process of galvanic corrosion. To improve brass resistance to dezincification, elements such as arsenic, antimony, or tin can be added to the alloy, which can inhibit zinc leaching of zinc by forming more stable protective layers [10].

The purpose of this study is to conduct a comprehensive assessment of the impact of chemical composition on the shrinkage behaviour and corrosion susceptibility of lead-free brass CB771 compared to the commonly used leaded brass CB770.

2. Methodology and materials

The study prepared a base sample of lead-free brass CB771 cast from ingots supplied by NordicBrass, along with modified variants. Based on preliminary analyses and studies, elements with the strongest influence on improving casting properties, such as zinc, tin, and aluminum, were selected, allowing the research to focus on their effects [13]. Modifications were made by adding the elements in pure form directly to the molten base alloy CB771, enabling the production of homogeneous samples with different chemical compositions. The aim of the study was to obtain detailed data on the effects of these alloying elements on shrinkage and corrosion resistance. For comparative analysis, a reference melt was also conducted using the commonly employed brass CB770, which contains approximately 1% lead. A total of seven castings with varying chemical compositions were produced under identical casting conditions, with a pouring temperature of 1030°C and a mold temperature maintained at 200°C. The detailed chemical composition of the tested alloys is presented in Table 1. The addition of zinc, tin, and aluminum to the CB771 alloy influenced the effective copper value (Cu_{eff}), calculated based on Guilett equivalents. These equivalents define the intensity and direction of each alloying element's effect relative to zinc, enabling the analysis of their specific impact on the alloy's shrinkage and corrosion resistance [12]. The samples underwent detailed examinations to assess how variations in the content of these elements affected shrinkage behavior and susceptibility to dezincification, providing insights into their roles in enhancing the alloy's functional properties.

Table 1.
Alloy composition measured on Bruker Q8 Magellan spectrometer

Name / Element		Cu [wt %]	Zn [wt %]	Pb [wt %]	Sn [wt %]	Al [wt %]	As [wt %]	Sb [wt %]	Cu_{eff} [wt %]
P1	CB771	63.13	36.10	0.087	0.008	0.488	0.036	0.037	61.67
P2	CB771↑Zn↑Sn	61.99	**37.00**	0.104	**0.268**	0.451	0.040	0.041	60.51
P3	CB770	62.78	35.37	0.729	0.099	0.709	0.087	0.007	60.99
P4	CB771↑Sn	63.13	35.83	0.090	**0.251**	0.491	0.036	0.038	61.54
P5	CB771↑Sn↑Al	63.09	35.73	0.086	**0.252**	**0.667**	0.036	0.036	60.94
P6	CB771↑Zn	62.09	**37.16**	0.087	0.008	0.483	0.035	0.035	60.66
P7	CB771↑Al	62.66	36.36	0.088	0.008	**0.694**	0.036	0.035	60.61

2.1. Dilatometric Analysis

The measurement setup, whose schematic is shown in Figure 1, was designed and constructed to record dimensional changes in the casting during solidification and cooling. The dilatometric analysis test rig comprises the following basic components: a permanent mould (1), anchors (6), displacement sensors (4), and thermal insulation sheathing (10). The test procedure involves

pouring molten brass through the thermal insulation sheathing (10) into the mould (1), where it surrounds the anchors (6).

During the test, the dimensional changes of the sample were recorded over time using precise displacement sensors. These sensors allowed for accurate tracking of displacements with an accuracy of 0.01 mm and a recording frequency was one per 0,1 second, enabling detailed data collection on the sample's behaviour throughout the solidification process. Simultaneously, the temperature of the sample was recorded using a thermocouple placed in the central part of the casting, allowing real-time monitoring of temperature changes. The recorded measurements made it possible to develop cooling rate curves, which depict the kinetics of temperature changes in the sample over time, as well as absolute and relative shrinkage curves, which quantitatively determine the reduction in sample dimensions relative to its initial dimensions.

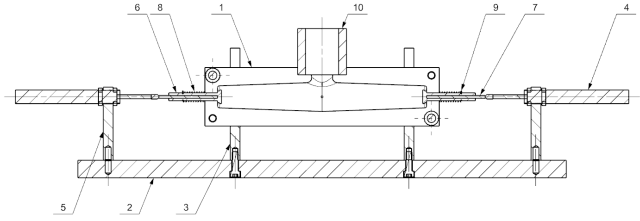

Fig. 1 Schematic of the test rig for dilatometric analysis. 1-Permanent mould, 2-base, 3-mould support, 4-displacement sensor, 5-displacement sensor support, 6-anchor, 7-quartz tube, 8-spring, 9-locking ring, 10-thermal insulation tube

2.2. Dezincification and microstructure

Samples were taken to test the dezincification resistance and microstructure from the central part of the casting gating system used for the dilatometric analysis. Measurement of dezincification levels of the CuZn alloys was carried out according to the standardized procedure specified in ISO-6509. Properly prepared samples, measuring 10x10x10 mm, were subjected to $CuCl_2$ exposure on a surface area of 100 mm² at a temperature of 75°C for 24 hours. After exposure, the samples were cleaned and prepared for measurement and metallographic analysis using an optical microscope equipped with a camera and image analysis software. The dezincification depth was measured along a 10 mm section, with 25 measurements taken and averaged to determine the mean dezincification value. One sample of each alloy was subjected to dezincification testing to ensure consistency in results.

3. Results and discussion

3.1. Dilatometric Analysis

Figure 2 presents the dilatometric curves of the brass alloys. At approximately 920°C, the solidification kinetics of all alloys are very high and similar across all samples, indicating an intense crystallization process. However, the shrinkage values for different samples are varied, indicating the influence of different alloying additives on their shrinkage processes.

As the temperature decreases from 900°C to around 800°C, the differences between the shrinkage curves become more pronounced. Samples with aluminium, zinc, and tin additives exhibit lower shrinkage values, indicating greater dimensional stability at higher temperatures.

The most significant differences in shrinkage kinetics between the samples are observed at high temperatures, where different alloying additives affect the shrinkage processes. At lower temperatures, the dilatometric curves of individual samples become more similar to each other.

The shrinkage curves can be correlated with the effective copper (Cu_{eff}) values for the individual samples. It has been observed that as Cu_{eff} values decrease, the shrinkage also decreases. The CB771 sample, which has the highest Cu_{eff} value of 61.67%, exhibits the largest shrinkage. Samples with aluminium additives, such as CB771Al and CB771SnAl, show lower shrinkage values. The CB770 sample, which contains lead, has a lower shrinkage. Samples CB771ZnSn and CB771Sn, enriched with tin, show greater dimensional stability and lower shrinkage, suggesting that tin stabilizes the solidification process. The CB771Zn sample, with zinc addition, has moderate shrinkage, indicating a moderate influence of zinc on the shrinkage processes. These differences are due to the different chemical compositions of the alloys.

Cu_{eff} values significantly affect the material's behaviour at high temperatures, as clearly seen in the dilatometric analysis. A decrease in Cu_{eff} values leads to a reduction in shrinkage, which may result from structural changes due to different alloying additives affecting the solidification process.

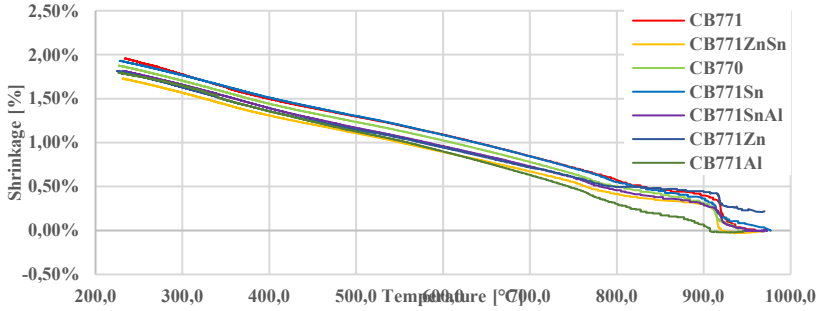

Fig. 2. Shrinkage curves of the investigated brasses

Based on the shrinkage values read from the dilatograms, it was possible to calculate the actual shrinkage coefficient αα, which characterizes the quantitative changes in the dimensions of the samples during cooling. The actual shrinkage coefficient is defined by Equation (1). Determining the actual shrinkage coefficient involves differentiating the shrinkage curve, which allows the determination of the rate of dimensional change rate of the sample as a function of temperature.

$$\alpha = \frac{1}{l}\frac{dl}{dT} \tag{1}$$

gdzie:
T – temperature [°C]
l – sample length [mm]

Figure 3 shows the developed plot of the shrinkage coefficient as a function of temperature for CB771 brass without alloying additives, in relation to the shrinkage curve of this alloy. This plot clearly illustrates how the intensity of shrinkage changes during the solidification and cooling of CB771 brass without additives.

Analysis of the shrinkage curves and the shrinkage coefficient α\alphaα of the CuZn alloys, taking into account the temperature values, provided essential information about the solidification and cooling parameters of the brasses studied. This analysis allowed for the identification and proper classification of critical points corresponding to phase transformations on the CuZn equilibrium diagram.

From the onset of solidification, point α1 reflects the maximum shrinkage effect resulting from intense structural changes associated with the transition β→α+β. The next significant point is α2 indicating the transformation α+β→α. Point α3 indicates the ordering transition of phase β→β'.

According to this procedure, the temperatures for all brasses tested were recorded, and the results are presented in Table 2.

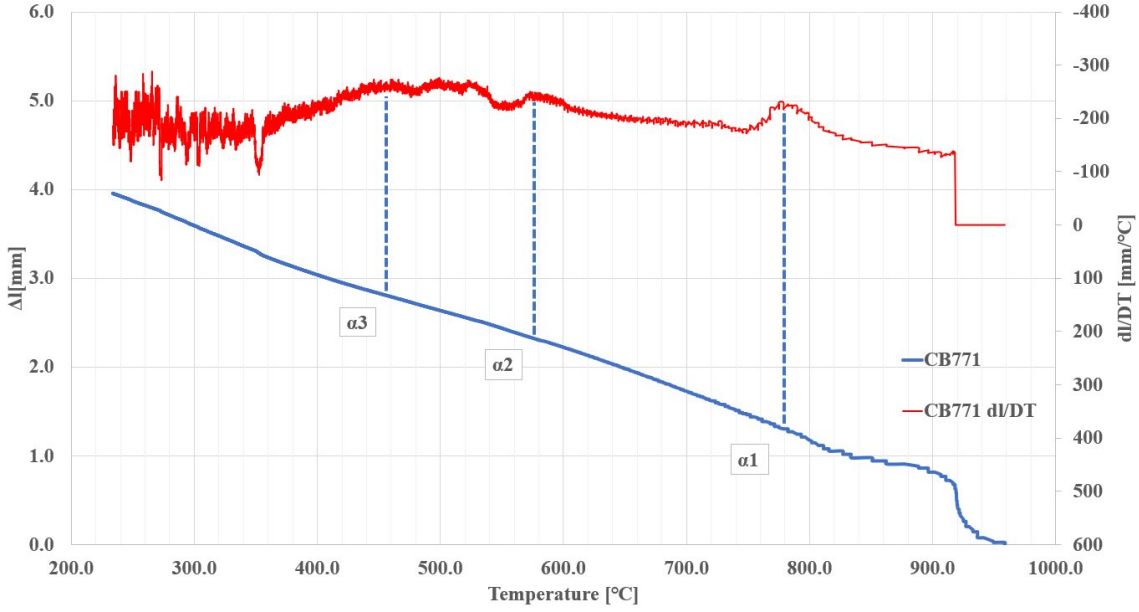

Fig. 3. The shrinkage coefficient graph in relation to the shrinkage curve of CB771 brass.

Table 2.
The shrinkage coefficient of the tested brasses.

	CB771		CB771ZnSn		CB770		CB771Sn		CB771SnAl		CB771Zn		CB771Al	
	Temp [°C]	dl/DT	Temp [°C]	dl/DT	Temp [°C]	dl/DT	Temp [°C]	dl/DT	Temp [°C]	dl/DT	Temp [°C]	dl/DT	Temp [°C]	dl/DT
α1	786	-0,224	782	-0,265	802,6	-0,225	802,5	-0,210	764,9	-0,231	765,6	-0,346	797,7	-0,187
α2	574	-0,238	-	-	-	-	-	-	-	-	-	-	-	-
α3	458	-0,262	459	-0,273	462,7	-0,254	462,7	-0,264	458,2	-0,233	447,9	-0,257	457,4	-0,248

The temperature for point α1, indicating the phase transition β → α + β, varies depending on the alloy composition, with the highest temperature observed for alloy CB770 (802.60°C) and the lowest for CB771SnAl (762.80°C). This indicates that the addition of different alloying elements affects the starting temperature of the β → α + β, transition, which can be crucial to optimize the casting process. The absolute shrinkage value at point α1 is the highest for the CB771 alloy without additives (1.25 mm), suggesting a greater tendency for volumetric changes during the β → α + β transition compared to the other alloys.

Point α2 was only for the CB771 alloy without alloying additives, indicating the occurrence of the α + β → α phase transition in this alloy. The temperature of this transition is 575.80°C, with an absolute shrinkage of 2.32 mm. The absence of this point in other alloys indicates a relatively low effective zinc

percentage in the CB771 alloy. The location of the α + β → α transition in the CuZn equilibrium system is shown in Figure 5.

For point α3 the transition temperatures are similar for the respective alloys, ranging between 446.80°C and 463.10°C. Absolute shrinkage at this point is highest for the CB771 alloy (2.80 mm), again indicating its greater tendency to volumetric changes. The smallest absolute shrinkage (at point α3) was observed for the alloy CB771Zn (2.55 mm).

The addition of Sn and Al appears to reduce absolute shrinkage compared to the base CB771 alloy. For example, CB771ZnSn and CB771SnAl have lower shrinkage values at point α1 compared to CB771. This may indicate a stabilizing effect of these additives on the solidification process.

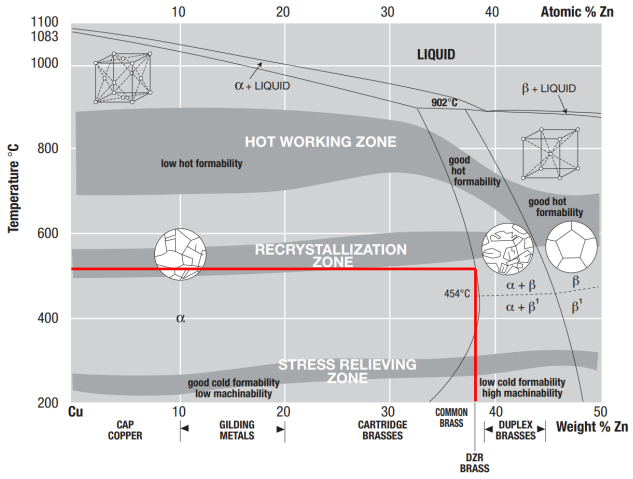

Fig. 4. The α + β → α transformation on the Cu-Zn equilibrium diagram [9]

3.2. Dezincification and microstructure

The microstructures presented in Figure 5 illustrate the characteristic dual-phase structure of CuZn alloys, where light grains of the α phase are visible against the darker β' phase. In particular, leaded brass CB770 exhibits significantly finer grain size compared to lead-free brass CB771 and its chemically modified variants. According to the data in Table 3, the average grain area for CB770 is 190.28 μm², while for CB771 with various alloying additives such as zinc, aluminum, and tin, these values are higher, reaching 864.79 μm² for CB771ZnSn, 648.83 μm² for CB771SnAl, 703.63 μm² for CB771Sn, and up to 1392.41 μm² for CB771Al.

The analysis of the microstructures confirms that alloying additives cause subtle but noticeable modifications in the structure of CB771 brass. For example, the addition of tin and zinc (CB771Sn, CB771ZnSn) reduces the average grain area, which can contribute to the improvement of the mechanical properties, correlating with the observed increase in the β' phase fraction, which is 65.55% for CB771Sn and 61.68% for CB771ZnSn. On the other hand, the addition of aluminum (CB771Al) significantly increases the grain size, which may affect other mechanical properties, as indicated by the β' phase fraction of 64.10%.

In summary, alloying additives significantly influence the microstructure and, consequently, the mechanical properties of CuZn alloys. This is evident in both the change in grain size and the fraction of individual phases, which can impact the hardness and tensile strength of these materials (Fig. 6).

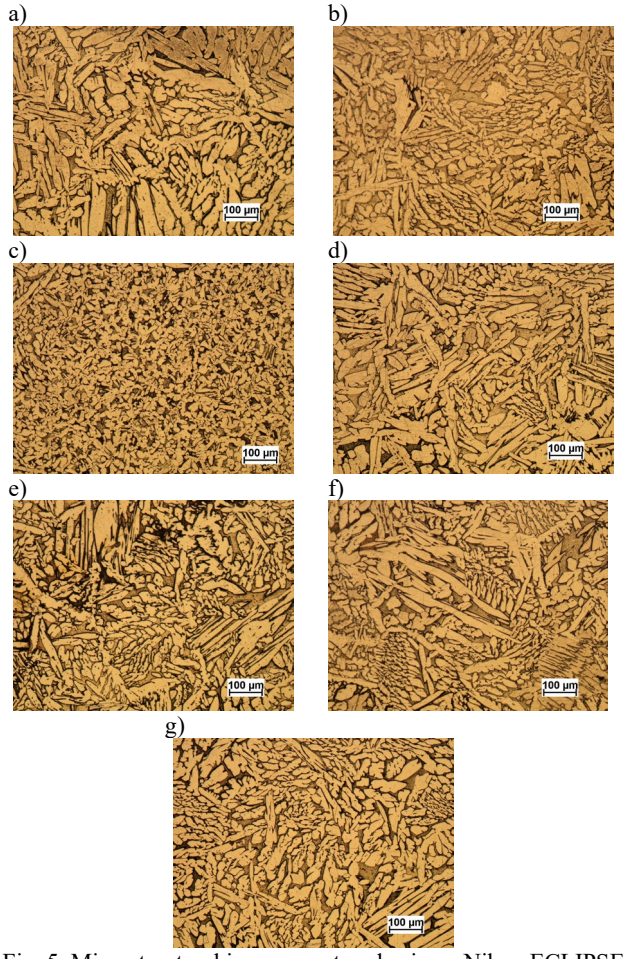

Fig. 5. Microstructural images captured using a Nikon ECLIPSE LV150 metallographic microscope: a) CB771, b) CB771ZnSn, c) CB770, d) CB771Sn, e) CB771SnAl, f) CB771Zn, g) CB771Al

Table 3.
Results of microstructure analysis using the NIS-Elements BR 3.10 software

	Average grain area [μm²]	Alpha phase fraction [%]	Hardness HB
CB771	746,22	62,50	85,5
CB771ZnSn	864,79	61,68	79,6
CB770	190,28	59,58	91,2
CB771Sn	703,63	65,55	78,8
CB771SnAl	648,83	54,28	83,5
CB771Zn	476,90	60,06	78,6
CB771Al	1392,41	64,10	82,5

The results of the quantitative assessment of the dezincification process for brass samples labeled CB770 and CB771, as well as for the alloys obtained resulting from the chemical modification of the

lead-free alloy, are presented in Figure 7. These data include both the average and maximum depths of dezincification after exposure to $CuCl_2$.

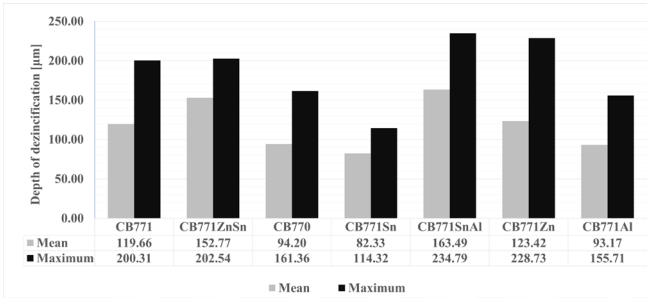

Fig. 7. Depth of dezincification determined in accordance with EN-ISO 6509

To illustrate the impact of $CuCl_2$ on the structure of the tested materials, representative microstructures of the samples exposed to this chemical are presented. Figure 8 shows microstructural images taken in polarized light, detailing the changes in microstructure that occurred as a result of exposure to the $CuCl_2$ solution.

These images clearly depict the transformations in the tested samples. The depth of dezincification is highlighted by a reddish color, allowing for easy identification of dezincified areas. This enables precise visualization and analysis of areas affected by dezincification due to $CuCl_2$ exposure, which is crucial to understanding the corrosion processes and structural changes in the tested materials.

Analyzing the results in the context of the PN-EN-ISO 6509 standard, which concerns brass resistance to dezincification, the focus was on the average dezincification values for each alloy tested. All samples exhibited a layered type of dezincification.

It was found that CB771, the base lead-free brass, has an average dezincification value of 119.66 µm at 38.33% Zn_{eff}, serving as a reference point for the other alloys. CB771ZnSn shows a slightly higher average dezincification value of 152.77 µm at 39.49% Zn_{eff}, suggesting a greater susceptibility to selective corrosion compared to base brass.

Leaded brass, CB770, has a significantly lower average dezincification value of 94.20 µm at 39.01% Zn_{eff}, suggesting a better resistance to dezincification compared to lead-free brass. On the other hand, CB771Sn has the lowest average dezincification value of 82.33 µm at 38.46% Zn_{eff}, making it the most resistant to dezincification among the alloys tested. This suggests that the addition of tin significantly increases resistance to dezincification.

The alloy CB771SnAl, which contains both tin and aluminum, has a higher average dezincification value of 163.49 µm at 39.06% Zn_{eff}, which is a lower result compared to CB771Sn. These findings suggest that the combination of aluminum and tin does not provide optimal resistance to dezincification, possibly due to the synergistic effect of both additives and the relatively high effective zinc content.

The CB771Zn alloy has an average dezincification value of 123.42 µm at 39.34% Zn_{eff}, which is slightly higher than that of the base brass, suggesting that zinc may slightly increase susceptibility to dezincification.

Meanwhile, CB771Al exhibits an average dezincification value of 93.17 µm at 39.28% Zn_{eff}, which is significantly lower than that of CB771SnAl. This indicates that aluminum can significantly improve resistance to dezincification, particularly when not combined with tin.

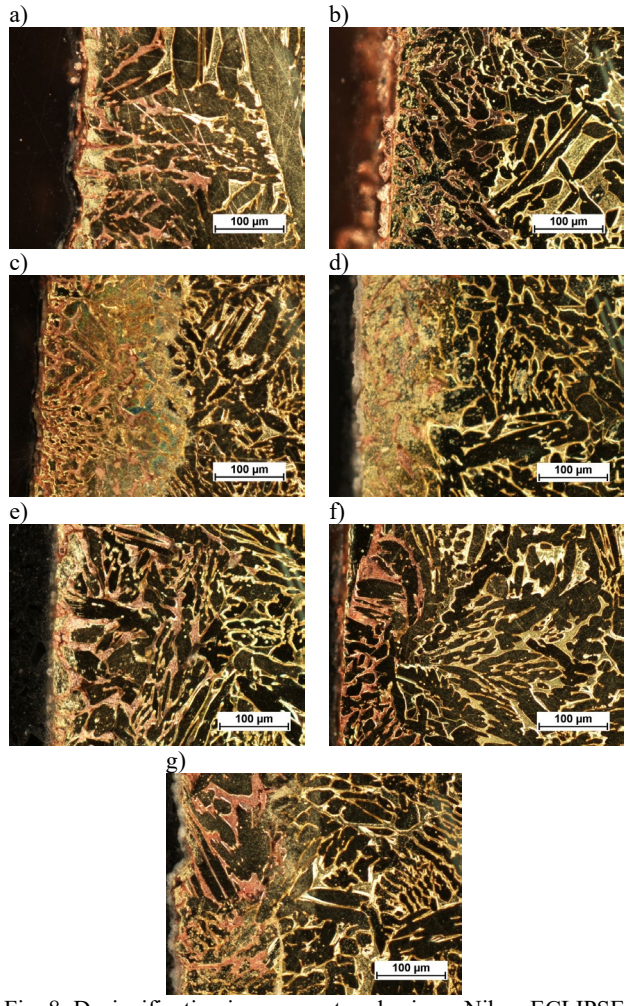

Fig. 8. Dezincification images captured using a Nikon ECLIPSE LV150 metallographic microscope equipped with NIS-Elements BR 3.10 software: a) CB771, b) CB771ZnSn, c) CB770, d) CB771Sn, e) CB771SnAl, f) CB771Zn, g) CB771Al

4. Statistical Analysis

The research results were subjected to statistical analysis using the "Nonlinear Estimation" module in STATISTICA 13.3 software. The NE module allows for the definition of virtually any type of regression model. The aim of the analysis was to determine the impact of the chemical composition of the brass alloys on the structural parameters and the results of dilatometric tests. The input data for this analysis were derived from Tables 1, 2, and 3, which contain detailed information on the chemical composition (Table 1), shrinkage coefficients at various transformation

temperatures (Table 2), and microstructural parameters such as average grain area and alpha phase fraction (Table 3).Of the tested hypotheses, five models were statistically significant or had a satisfactory level of significance in terms of the volume of data which was assumed as less than 0,3. The statistical parameters of their evaluation are presented in Table 4, while the forms of the dependencies, including the coefficient values and their graphical representations, are shown in Figure 9. On the graphs, the regression functions are provided, with data points marked with * representing values calculated from these functions, and points without * corresponding to the actual measured values. The regression model for "Shrinkage"=f(Zn_{eff}) shows a very strong linear relationship (Figure 8a). The high coefficient of determination (R^2) indicates that the model explains most of the variability in the "Shrinkage" variable. The model is statistically significant, as confirmed by the very low p-value. This model can be very useful for predicting shrinkage values based on Zn_{eff}.

The regression model for the "Alpha phase fraction"=f(Zn_{eff}) shows a moderate second-degree nonlinear relationship between the variables. However, the negative adjusted R^2 and a p-value greater than 0.05 indicate that the model is not statistically significant, but it can be assumed that there is an influence of Zn_{eff} on the percentage of the alpha phase in the brass structure.

The regression model for "Average grain area"=f(Zn) shows a strong second-degree nonlinear relationship between the variables, a high R^2, and a p-value < 0.05, confirming the statistical significance of the model. An alternative model for this relationship, "Average grain area"=f(Sn), indicates the existence of such a relationship but with less strength, as indicated by the negative adjusted R^2 and a p-value > 0.05. This model can be used auxiliary in conjunction with "Average grain area"=f(Zn) for predicting structural parameters, but statistically proving a significant synergistic effect of Zn and Sn on "Average grain area" did not yield satisfactory results.

The regression model for α1=f(Zn) shows a strong nonlinear relationship between the variables, a high coefficient of determination (R^2), and a p-value < 0.05, confirming the statistical significance of the model.

The most effective and precise regression model was obtained for the variable "Shrinkage." The statistical parameters obtained in the analysis for the dependent variables "Alpha phase fraction" "Average grain area" and α1 suggest a dependence on the chemical composition, but to confirm these, the number of data points in the analysed matrix of results should be increased.

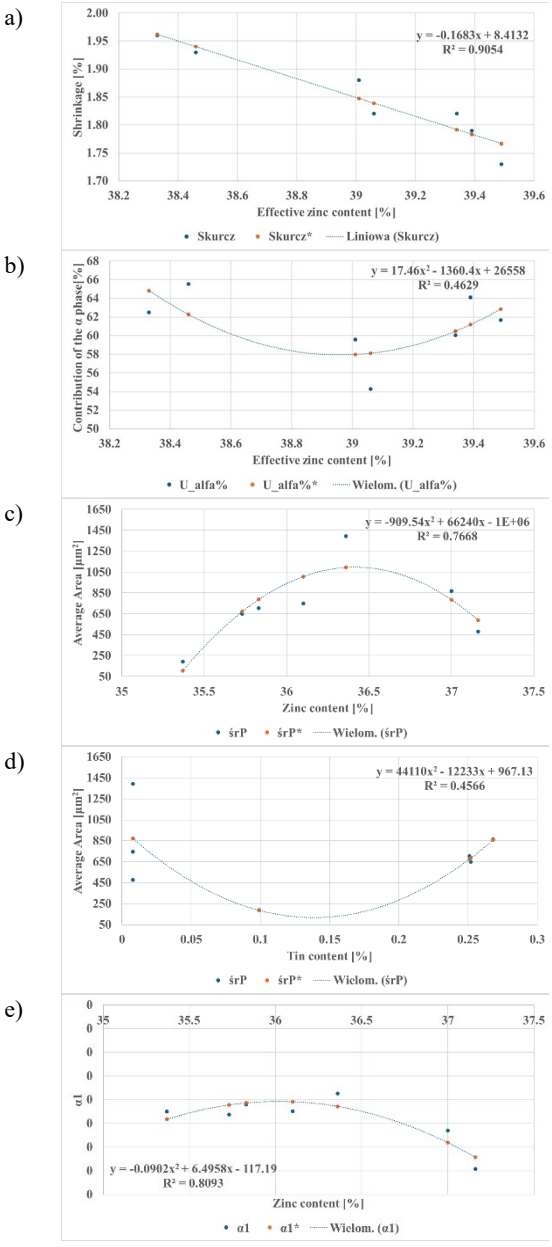

Fig. 9. Regression models with marked regression functions

Table 4.
Statistical values for obtained models of dependencies

Dependent Variable	Independent Variable	R	Adjusted R^2	R^2	Fischer Test F	Significance level p	Standard error of estimation
Shrinkage	Zn_{eff}	0,951546	0,886527	0,905439	F(1,5)=47,876	0.00097	0.02721
Alpha phase fraction	Zn_{eff}	0,683038	0,194329	0.466288	F(2,4)=1,7236	0.28849	3.298
Average grain area	Zn	0,875661	0,650172	0,7667814	F(2,4)=6,5428	0.05439	218.49
Average grain area	Sn	0,675699	0,184854	0,456569	F(2,4)=1,6804	0.25392	333.52
α1	Zn	0,899605	0,739358	0,809290	F(2,4)=8,487	0.03837	0.2773

5. Conclusions

Brass samples with modified chemical compositions exhibit varied dilatometric properties directly related to the presence of additives such as zinc, aluminum, and tin. Dilatometric analysis indicates that these additives reduce the shrinkage of the casting at higher temperatures, reflecting greater dimensional stability of these alloys. Specifically, the addition of zinc, aluminium, and tin reduces shrinkage, potentially improving mechanical properties. The shrinkage decreases with the effective copper content (Cu_{eff}), which can be observed in samples with higher levels of alloying additives.

Corrosion resistance, including resistance to dezincification, is a key aspect of the tested CuZn alloys. Studies conducted show that tin and aluminium additives significantly improve resistance to dezincification, which is particularly important for materials used in contact with drinking water. The CB770 alloy (leaded brass) shows better dezincification resistance than most lead-free CB771 alloys, but the addition of tin (CB771Sn) increases this resistance even compared to leaded brass.

Among the alloys tested, CB771Sn exhibits the highest resistance to dezincification, suggesting that tin is particularly effective in this context. On the contrary, the CB771SnAl alloy, despite its tin content, shows a poorer resistance to dezincification, likely due to a synergistic effect with aluminum.

Microstructural analysis revealed that the alloying additives cause changes in the brass structure, increasing grain size and the proportion of the β' phase. This can result in improved mechanical properties and material hardness.

In summary, studies showed that modifications in the chemical composition of lead-free brasses significantly impact their dilatometric properties and resistance to dezincification. Particularly beneficial effects were achieved with the addition of tin, which significantly enhances the selective corrosion resistance, and aluminum, which stabilizes the shrinkage processes of the alloys. These findings are important for the further development and optimization of lead-free brass alloys in applications requiring high corrosion resistance and dimensional stability.

Acknowledgement

The research was funded by the Ministry of Science and Higher Education as part of the VI edition of the "Implementation Doctorate" program conducted at the Doctoral School of the Silesian University of Technology in the Department of Foundry Engineering.

References

[1] Zoghipour, N., Tascioglu, E., Celik, F. & Kaynak, Y. (2022). The influence of edge radius and lead content on machining performance of brass alloys. *Procedia CIRP.* 112, 274-279. https://doi.org/10.1016/j.procir.2022.09.084.

[2] Hansen, A. (2019). Bleifreier rotguss als armaturen-und installationswerkstoff in der trink wasser installation. *METALL Forschung*. 73(11), 452-455.

[3] Stavroulakis, P., Toulfatzis, A., Pantazopoulos, G. & Paipetis A. (2022). Machinable leaded and eco-friendly brass alloys for high performance manufacturing processes: a critical review. *Metals.* 12(2), 246, 1-31. https://doi.org/10.3390/met12020246.

[4] Schultheiss, F., Johansson, D., Bushlya, V., Zhou, J., Nilsson, K. & Ståhl, J-E. (2017). Comparative study on the machinability of lead-free brass. *Journal of Cleaner Production.* 149, 366-377. https://doi.org/10.1016/j.jclepro.2017.02.098.

[5] Johansson, J., Alm, P., M'Saoubi, R., Malmberg, P., Ståhl, J-E. & Bushlya, V. (2022). On the function of lead (Pb) in machining brass alloys. *Journal of Advanced Manufacturing Technology.* 120(11), 7263-7275. https://doi.org/10.1007/s00170-022-09205-0.

[6] Umwelt Bundesamt. (2024). *Acceptance of metallic materials used for products in contact with drinking water, 4MS Common Approach Part B "4MS Common Composition List"*. Retrieved July, 12, 2022 from http://www.umweltbundesamt.de/en/topics/water/drinking-water/distributing-drinking-water/guidelines-evaluation-criteria.

[7] Directive (EU) 2020/2184 of the European Parliament and of the Council of 16 December 2020 on the quality of water intended for human consumption, Dz.U.L 435/1 of 23.12.2020.

[8] Studnicki, A., Jura, S. & Kilarski, J. (1998). The investigation of chromium cast iron on casting dilatometer DO-01/P.Śl. *Solidification of Metals and Alloys.* 38, 223-228 (in Polish).

[9] Jacobsson, D., Däcker, C.-Å., Sundberg R. & Rod, O. (2010). *A general guide for failure analysis of brass*. Stockholm. Sweden: Swerea KIMAB, 2010.

[10] Jones, D.A. (1992). *Dealloying and dezincification. in principles and prevention of CORROSION*. New York: Macmillaian Publishing Company.

[11] Claesson, E. & O. Rod, O. (2016). The effect of alloying elements on the corrosion resistance of brass. *Materials Science and Technology*. 32(17), 1794-1803. https://doi.org/10.1080/02670836.2016.1254925.

[12] Górny, Z. (1992). *Non-ferrous metal casting alloys.* Wydawnictwa Naukowo Techniczne. ISBN: 83-204-1270-6. (in Polish).

[13] Radzioch, G., Bartocha, D. & Kondracki, M. (2023). Experimental and numerical comparison of lead-free and lead-containing brasses for fixture application. *Archives of Foundry Engineering*. 23(3), 124-132. DOI: 10.24425/afe.2023.146672.